Theor Chem Acc (2012) 131:1193
DOI 10.1007/s00214-012-1193-z

REGULAR ARTICLE

Scalar-relativistic 5f-in-core pseudopotentials and core-polarization potentials for trivalent actinides: calibration calculations for Ac^{3+}, Cm^{3+} and Lr^{3+} complexes

Daniel Weißmann · Michael Dolg

Received: 15 July 2011 / Accepted: 23 August 2011 / Published online: 3 March 2012

Abstract The performance of recently proposed 5f-in-core pseudopotentials for the trivalent actinides was investigated in calculations for model complexes $An^{3+}L^{n-}$ for three selected actinides (An^{3+} = Ac^{3+}, Cm^{3+}, Lr^{3+}) and eight simple ligands with atoms from the first three periods of the table of elements (L^{n-} = F^-, Cl^-, OH^-, SH^-, CO, NH_2^-, H_2O, H_2S, NH_3). Results of Hartree-Fock and Coupled Cluster with singles, doubles and perturbative triples calculations using basis sets of quadruple-zeta quality are compared to corresponding reference data obtained with scalar-relativistic energy-adjusted 5f-in-valence small-core pseudopotentials. The inclusion of core-polarization potentials in the 5f-in-core pseudopotential calculations and corrections of the basis set superposition error by the counterpoise correction leads to very good agreement between the 5f-in-valence and 5f-in-core pseudopotential results for bond lengths, bond angles and binding energies. Results from 5f-in-core pseudopotential calculations using different density functionals also show reasonable agreement with the more rigorous Coupled Cluster results. It is argued that the An 5f rather than the An f population is a useful criterion for the applicability of a specific An 5f-in-core pseudopotential.

Keywords Actinides · Pseudopotentials · Core-polarization potentials · Calibration

1 Introduction

Prior to the twentieth century almost nothing was known about the properties and chemistry of the actinides, mainly because of their radioactivity and toxicity, although already 1,833 flourescenting uranyl compounds were described [1]. Only the rapid technological evolution in the twentieth century opened the possibility to analyze and also to prepare the radioactive actinides. Most of these elements were generated and discovered by bombardment of heavy atoms with neutrons in nuclear reactors or as result from nuclear detonations. However, nowadays, most of the actinides are left as an object of fundamental research.

Beyond the fundamental research, the biggest part of actinide chemistry concentrates on disposal and partitioning of nuclear waste [2]. Actinides and their compounds are due to their complicated synthesis, isolation and handling a costly and delicate part of preparative and analytical chemistry. Quantum chemical calculations are a useful tool to support the experimental investigations and can help to better understand actinide chemistry [3 –6].

Significant relativistic effects [7], the high number of electrons as well as electron correlation pose big challenges for the computational methods, which are used to investigate actinide chemistry. For first-principles studies of actinides especially the complexities arising from partially occupied f shells are cumbersome and motivate the development of approximate schemes based on chemical intuition [3, 8]. The application of pseudopotentials (PPs) is a widely used way of approximation to cope with some of these problems successfully. Within this method, the

Electronic supplementary material The online version of this article (doi:10.1007/s00214-012-1193-z) contains supplementary material, which is available to authorized users.

D. Weißmann · M. Dolg (✉)
Institute for Theoretical Chemistry,
University of Cologne, Greinstr. 4,
50939 Cologne, Germany
e-mail: m.dolg@uni-koeln.de

D. Weißmann
e-mail: daniel.weissmann@uni-koeln.de

explicit quantum mechanical treatment is restricted to the chemically relevant valence electrons, including possibly also electrons in chemically noninert semi-core orbitals, thus significantly reducing the computational effort with respect to an all-electron treatment. PPs take implicit account of relativistic effects, since the valence model Hamiltonian parameters are properly adjusted to relativistic reference data. With modern pseudopotentials and adequate computational methods, just a few percent deviation from experimental data and relativistic all-electron results can be achieved [9, 10], even for f elements [6, 11–13].

For f elements, two kinds of energy-consistent PPs with different core definitions have been published. On one hand, there are f-in-core PPs (large-core PPs, LPPs) [14–20], where one has one PP for each fixed f^n subconfiguration of a given atom, i.e. for each oxidation state one has a corresponding PP. The f-in-core PPs avoid many difficulties due to the open f shell, and despite their approximate nature is an efficient computational tool for those actinide/lanthanide compounds, where the f shell does not significantly contribute to bonding. Hence, calculations even on large molecules also containing several f elements become feasible. On the other hand, there are the more standard and computationally more costly f-in-valence PPs (small-core PPs, SPPs) [21–26] with a large valence space, i.e. a small core avoiding frozen-core errors. For example, the 5f-in-core PP for Cm^{3+} treats just the $6s^2$ $6p^6$ electrons explicitly, whereas for the corresponding 5f-in-valence PP, the $5s^2$ $5p^6$ $5d^{10}$ $5f^7$ $6s^2$ $6p^6$ electrons are in the valence space. In order to enhance the quality of results from f-in-core PP calculations, core-polarization potentials (CPPs) [27, 28] were used [16, 19]. They account for static and dynamic (core-valence correlation) polarization of the PP core and are particular important for LPPs as the f-in-core PPs for lanthanides and actinides.

In case of U, it was frequently observed that a SPP approach (32 valence electrons) is superior to a LPP approach with an explicit treatment of the 5f shell (14 valence electrons) [29–32]; however, it was also claimed that the LPP approach still gives good results when the oxidation state of U does not change [33]. The latter finding is supported by all-electron (AE) Dirac-Hartree-Fock frozen-core results [8]. When freezing an 78-electron core of neutral U in its $5f^3$ $6d^1$ $7s^2$ ground-state configuration, i.e. treating U as a 14-valence electron system, the errors in the energy differences to U^+ $5f^3$ $7s^2$, U^{2+} $5f^3$ $7s^1$ and U^{3+} $5f^3$ are below 0.001 eV, whereas corresponding errors for configurations with $5f^2$, $5f^1$ and $5f^0$ subconfigurations are larger than 0.06, 0.30 and 0.73 eV, respectively. Clearly, the good atomic results obtained for a fixed explicitly treated $5f^3$ subconfiguration alone do not guarantee a similar good performance of a U 14-valence electron PP in molecular calculations, but they are a necessary prerequisite. Since the LPPs applied here even go one step further compared to the ones tested in these studies, i.e. the open 5f shell is included in the PP core, it is interesting to check the performance of these LPPs for structural and energetic data.

The 5f-in-core LPPs for actinides were initially tested for $An^{3+}H_2O$ complexes and for trifluorides AnF_3 at the Hartree–Fock (HF) level by comparing to corresponding SPP results for VXZ (X = D, T, Q) basis sets [18]. The mean absolute (relative) deviations in the An–O and An–F bond distances were 0.01 Å (0.6%) and 0.03 Å (1.4%), respectively. The corresponding deviations for the binding energies were 0.08 eV (2%) and 0.09 eV (2%). The application of CPPs in connection with LPPs was later found to reduce the deviations in the An–F bond distances of the trifluorides further to 0.01 Å (0.5%). The deviations in the ionic binding energies decreased from 0.51 eV (1.1%) to 0.24 eV (0.5%) [34]. The LPPs were also successfully used in a number of applications [35–40]. However, quite large differences of 0.08–0.40 and 0.18–0.29 Å in U-ring and U–CO distances, respectively, were found in U(III) complexes $Cp'_3U(CO)$ ($Cp' = C_5H_{5-n}(CH_3)_n$) between LPP and SPP results [41]. Since the LPP calculations in contrast to SPP calculations yield a too weak bonding, an influence of the 5f shell on both U–Cp' and U–CO bonding is assumed. As pointed out, e.g. in the first publication on 5f-in-core actinide PPs, the approach cannot deal with cases where the 5f shell gets significantly involved in covalent bonding [18]. Whereas the 5f-in-core PPs still allow a charge transfer from the ligand to the partially occupied 5f shell, the approach has to fail for a charge transfer in the opposite direction. As will be discussed in this work, test calculations on $Cp_3U(CO)$ ($Cp = C_5H_5$) in fact indicate that there are less than three unpaired electrons in the U 5f shell and thus the usage of a U $5f^3$-in-core PP is inappropriate. Smaller, but also noticeable differences of 0.04–0.09 Å in averaged bond distances between LPP and SPP averaged An–N distances were observed for 1:3-complexes of Np^{3+}, Pu^{3+}, Am^{3+} and Cm^{3+} with alkylated 2,6-ditriazinylpyridine [42].

We note that except for the initial test calculations on the trifluorides [34], the studies mentioned above do not take into account core-polarization effects by combining the LPPs with CPPs. Therefore, in the present contribution, the 5f-in-core LPPs and corresponding CPPs for the trivalent Ac, Cm and Lr are tested with the ionic ligands F^-, Cl^-, OH^-, SH^- and NH_2^-, as well as the neutral ligands CO, H_2O, H_2S and NH_3 using the HF approach and the Coupled Cluster method with single, double and perturbative triple excitations (CCSD(T)). Since the 5f-in-core PPs were derived in the framework of HF calculations, the transferability to density functional theory (DFT) calculations is an issue. Moreover, most electronic structure codes

cannot deal with CPPs. Therefore, corresponding 5f-in-core PP results obtained without CPPs for three different density functionals are also presented and discussed.

2 Method

The applied PPs, basis sets and CPPs used in this contribution were previously published [18, 22, 24, 34]. The method of relativistic energy-consistent pseudopotentials (PPs) is described in recent reviews [6, 11] and will here only be outlined briefly.

For a system with n valence electrons and N nuclei with charges Q, the valence-only model Hamiltonian is given as

$$\hat{H}_v = -\frac{1}{2}\sum_{i=1}^{n_v}\Delta_i + \sum_{i<j}^{n_v}\frac{1}{r_{ij}} + \sum_{I=1}^{N}\sum_{i=1}^{n_v}\hat{V}_{cv}^{I}(\mathbf{r}_{iI}) + \sum_{I<J}^{N}\frac{Q_I Q_J}{R_{IJ}}. \tag{1}$$

The indices i and j are for electrons and I and J are nuclear indices. $\hat{V}_{cv}^{I}(\mathbf{r}_{iI})$ is the one-electron potential due to center I describing the interaction of the valence electrons with the core. With the leading core-electron attraction, term $\hat{V}_{cv}^{I}(\mathbf{r}_{iI})$ has the overall form

$$\hat{V}_{cv}^{I}(r_{iI}) = \sum_{i=1}^{n_v}\left[-\frac{Q_I}{r_{iI}} + \hat{V}_{I}^{PP}(\mathbf{r}_{iI})\right]. \tag{2}$$

Within a semilocal approximation, the scalar-relativistic PP $\hat{V}_{I}^{PP}(\mathbf{r}_{iI})$ contains for each l value a linear combination of radial Gaussian functions

$$\hat{V}_{I}^{PP}(\mathbf{r}_{iI}) = \sum_{l=0}^{l_{\max}}\sum_{k} A_{lk}^{I}\mathrm{e}^{-a_{lk}^{I}r_{iI}^{2}}\hat{P}_{l}^{I}, \tag{3}$$

with $\hat{P}_{l}^{I}$ denoting the projection operator

$$\hat{P}_{l}^{I} = \sum_{m_l=-l}^{l}|lm_l, I\rangle\langle lm_l, I| \tag{4}$$

with respect to angular momentum l at core I.

For the scalar-relativistic 5f-in-core Wood–Boring (WB) [43] PPs for the trivalent actinides ($5f^n$, $n = 0$ for Ac, $n = 7$ for Cm, $n = 14$ for Lr) [18], the 1s–5f shells are included in the PP core and only 11 valence electrons are treated for the neutral atom, i.e. the core charge is $Q = 11$. Two types of radial potentials with $l = 3$, V_1 and V_2 model 5f shells which can and cannot accommodate an additional electron, respectively. The potential V_1 and V_2 are linearly combined to give the applied f potential as follows [18]:

$$V = \left(1 - \frac{m}{14}\right)V_1 + \frac{m}{14}V_2. \tag{5}$$

Here, m denotes the integral number of electrons in the 5f orbitals kept in the core. For a $5f^0$ occupation $V = V_1$ and for a $5f^{14}$ $V = V_2$ corresponds to the exact potential, respectively.

The CPPs [34] used here are of the form suggested by Müller et al. [27, 28]

$$V_{CPP} = -\frac{1}{2}\sum_{I}\alpha_I\mathbf{f}_I^2 \tag{6}$$

Here, α_I denotes the dipole polarizability of the PP core I. The electric field $\mathbf{f}_I$ at this core induced by all other cores or nuclei with charges Q_I and all electrons is given as

$$\mathbf{f}_I = -\sum_{i}\frac{\mathbf{r}_{iI}}{r_{iI}^3}F(r_{iI},\delta_I) + \sum_{J\neq I}Q_I\frac{\mathbf{r}_{JI}}{r_{JI}^3}F(r_{JI},\delta_I). \tag{7}$$

The applied dipole polarizabilities α_I of Ac^{3+}, Cm^{3+} and Lr^{3+} are 0.8982, 2.3242 and 3.7501, respectively. The cutoff function F is given as

$$F(r_{iI},\delta_I) = 1 - \mathrm{e}^{-\delta_I r_{iI}^2} \tag{8}$$

and the corresponding cutoff parameters δ_I of Ac^{3+}, Cm^{3+} and Lr^{3+} are 0.8727, 0.5712 and 0.2696, respectively [34]. The trivalent LPPs and CPPs were used in combination with (7s6p5d2f1g)/[5s4p3d2f1g] basis sets [18], and the corresponding scalar-relativistic 5f-in-valence Wood-Boring-adjusted small-core pseudopotentials (SPPs) with 60 core electrons [22] were used in combination with the segmented contracted (14s13p10d8f6g)/[10s9p5d4f3g] basis sets [26]. For the ligands, augmented correlation-consisted polarized valence quadruple-ζ basis sets (aug-cc-pVQZ) [44] were applied.

In order to reduce the computational effort, some orbitals were frozen at the CCSD(T) level. Within the SPP calculations for the actinide ions An^{3+}, the 5s, 5p and 5d orbitals were frozen, so just the remaining 6s, 6p and 5f electrons were correlated. For F^-, OH^-, CO, NH_2^-, H_2O and NH_3, the 1s orbitals were frozen, so that the 2s and 2p electrons are correlated. Analogously for Cl^-, H_2S and SH^-, just the 3s and 3p electrons were correlated, i.e. the 1s, 2s and 2p orbitals were frozen. Thus for all ligands, the eight valence electrons were correlated. Additional LPP calculations were performed with the BP86 [45, 46], B3LYP [47–50] and PBE0 [51] density functionals.

In this contribution, the structures of all complexes $An^{3+}L^{n-}$ and polyatomic ligands L^{n-} (n = 0, 1) were optimized at the HF and CCSD(T) level [52] for the LPP + CPP and SPP Hamiltonians using the MOLPRO 2006.1 program system [53]. Additional LPP calculations were performed at the DFT level. In the SPP calculations for the open-shell Cm systems, the resticted HF and CCSD(T) variants (RHF, RCCSD(T)) were applied [54]. The symmetries available in MOLPRO are restricted to D_{2h}

and subgroups. Thus, for the free ligands, except for ammonia, as well as the di- and tri-atomic actinide complexes, C_{2v} symmetry was imposed. All other complexes, as well as ammonia, were optimized imposing C_s symmetry.

3 Results and discussion

In the following, the results for binding energies D_e and actinide-ligand distances R_e from HF and CCSD(T) calculations using 5f-in-valence SPPs and 5f-in-core LPPs and CPPs will be presented. More extensive tables with additional data are given in the supplementary material. In the following, we discuss di- and triatomic systems, and tetra- and pentatomic complexes separately, due to a slightly different usage of the Boys-Bernardi counter-poise correction (CPC) [55] for correcting a possible basis set superposition error (BSSE). In case of the LPPs, the maximum CPC on the binding energy was 0.3 kJ mol^{-1} (<0.1%) for $Lr^{3+}NH_2^-$ at the HF level and 5.2 kJ mol^{-1} (1.8%) for $Ac^{3+}H_2S$ at the CCSD(T) level. In case of the SPPs, the corresponding values are 0.7 kJ mol^{-1} (<0.1%) for $Lr^{3+}NH_2^-$ at the HF level and 33.9 kJ mol^{-1} (1.6%) for $Ac^{3+}NH_2^-$ at the CCSD(T) level. Whereas at the HF level, the CPC amounts to at most 0.04 and 0.13% of the binding energy for LPPs and SPPs, respectively, much larger corresponding corrections of up to 1.9 and 9.7%, both for $Ac^{3+}H_2S$, are observed at the CCSD(T) level. It has to be noted, however, that the CPC at the CCSD(T) level for the Cm and Lr systems is between 10 and 20 kJ mol^{-1} smaller than for the Ac complexes. Moreover, in case of Ac, it was shown that the usage of a generalized contraction scheme reduces the BSSE significantly [26]. Nevertheless, the substantially smaller BSSE at the wavefunction-based correlated level is one advantage of the f-in-core LPP approach.

3.1 Di- and triatomic systems

For the di- and triatomic complexes $An^{3+}L^{n-}$ ($An^{3+} = Ac^{3+}$, Cm^{3+}, Lr^{3+}; $L^{n-} = F^-$, Cl^-, OH^-, SH^-, CO), the CPC could be taken into account during the geometry optimizations by minimizing the interaction energy defined as

$$\Delta E_{AL} = E_{AL}^{AL} - E_A^{AL} - E_L^{AL}, \quad (9)$$

where $A = An^{3+}$ and $L = L^{n-}$. Here, the subscript denotes the calculated systems, whereas the superscript denotes the applied basis sets. The evaluation is straightforward for the diatomic systems, where at every point of the geometry optimization procedure the energies of the fragments calculated in the complex basis set (E_A^{AL}, E_L^{AL}) are subtracted from the energy of the complex (E_{AL}^{AL}). For the diatomic ligands, E_L^{AL} was evaluated using the equilibrium structure of the free ligand. The distance between the coordinating O or S center of the ligand and the metal center hosting the ghost basis set was taken from the actual geometry used to evaluate E_{AL}^{AL}. The evaluation of the CPC in this way is motivated by our main interest in the metal-ligand distance and not in the interatomic distance in the diatomic ligands. The calculated An-L bond distances and binding energies are listed for the HF and CCSD(T) level in Tables 1 and 2, respectively.

3.1.1 Actinide-ligand bond lengths

The calculated LPP + CPP HF bond lengths for Ac–L, Cm–L and Lr–L deviate form the SPP HF results by at most 0.021 Å (1.1%, for $Lr^{3+}F^-$). The LPP + CPP results for Ac and Lr are slightly too short, whereas those for Cm are slightly too long. On average, the deviation for all 15 molecules is 0.011 Å (0.5%). At the LPP + CPP CCSD(T) level, the bond distances deviate from the SPP CCSD(T) values by at most 0.031 Å (1.6%, for $Cm^{3+}OH^-$). Again the LPP + CPP results for Ac and Lr are usually somewhat too short, and those for Cm too long. The average deviation is 0.014 Å (0.6%). We note that the comparisons made here are not completely accurate: the CPP used in the LPP approach describes implicitly both static and dynamic core polarization, whereas at the SPP HF level, only the static core polarization is explicitly accounted for.

Overall the LPPs of Ac and Lr perform somewhat better than the one of Cm, i.e. on average the deviations for all five ligands at the HF and CCSD(T) level amount to 0.4, 0.8 and 0.5% for Ac, Cm and Lr, respectively. The overall agreement between LPP + CPP and SPP results is also somewhat better for the ligands with elements from period three than with those from period two. The corresponding average deviations are 0.8, 0.4, 0.7, 0.4 and 0.5% for F^-, Cl^-, OH^-, SH^- and CO, respectively. The shorter bond distances of the period two systems cause the inner part of the PP to be probed more than it is the case for the period three systems exhibiting longer bond distances. It should be noted that the errors of the LPP + CPP approach are clearly smaller than those occuring, e.g. for post-d main group element LPPs [56].

The actinide contraction at the SPP level measured as the difference between the Ac and Lr bond distances is reproduced by the LPP approach with an accuracy better than 0.008 Å at the HF level and 0.019 Å at the CCSD(T) level. The size of the contraction is intermediate (0.14–0.22 Å) for F^-, Cl^-, HO^- and HS^-, and large (0.35 Å) for CO. The size of the contraction follows the order CO $\gg$ $HS^- > Cl^- > HO^- > F^-$, obeying roughly

Table 1 Ac^{3+}–L^{n-} ($n = 0, 1$) bond lengths R_e (in Å) and binding energies D_e (in kJ · mol^{-1}) from HF calculations using LPPs + CPPs as well as from SPP calculations for di- and triatomic systems

An^{3+}	L^{n-}	R_e		$\frac{\Delta R_e}{R_e(\mathrm{SPP})}$	D_e		$\frac{\Delta D_e}{D_e(\mathrm{SPP})}$
		LPP	SPP		LPP	SPP	
Ac^{3+}	F^-	2.005	2.018	−0.64	1,962.9	1,947.8	0.78
	Cl^-	2.497	2.505	−0.32	1,745.6	1,737.0	0.50
	HO^-	2.027	2.037	−0.49	2,085.1	2,070.4	0.71
	HS^-	2.499	2.507	−0.32	1,758.7	1,750.1	0.49
	CO	2.899	2.910	−0.38	152.3	149.7	1.74
m.p.d.				0.43			0.84
Cm^{3+}	F^-	1.932	1.925	0.36	2,080.5	2,078.1	0.12
	Cl^-	2.371	2.367	0.17	1,904.2	1,891.7	0.66
	HO^-	1.942	1.932	0.52	2,224.1	2,225.3	−0.05
	HS^-	2.364	2.361	0.13	1,922.4	1,910.3	0.63
	CO	2.681	2.691	−0.37	206.6	199.9	3.35
m.p.d.				0.31			0.96
Lr^{3+}	F^-	1.862	1.883	−1.12	2,170.6	2,145.5	1.17
	Cl^-	2.292	2.305	−0.56	2,010.9	1,985.5	1.28
	HO^-	1.868	1.883	−0.80	2,324.6	2,302.5	0.96
	HS^-	2.276	2.287	−0.48	2,019.3	1,994.1	1.26
	CO	2.546	2.564	−0.70	253.0	247.9	2.06
m.p.d.				0.73			1.35

The CPC was applied during the structure optimizations. The relative deviations $\frac{\Delta R_e}{R_e(\mathrm{SPP})}$ and $\frac{\Delta D_e}{D_e(\mathrm{SPP})}$ are given in %. The mean (absolute) percentage deviation (m.p.d.) is given for the differences between LPP and SPP results

Basis sets: LPP (7s6p5d2f1g)/[5s4p3d2f1g]; SPP (14s13p10d8f6g)/[10s9p5d4f3g]; H, O, Cl, S, F contracted aug-cc-pVQZ

Table 2 As Table 1, but for RCCSD(T) results

An^{3+}	L^{n-}	R_e		$\frac{\Delta R_e}{R_e(\mathrm{SPP})}$	D_e		$\frac{\Delta D_e}{D_e(\mathrm{SPP})}$
		LPP	SPP		LPP	SPP	
Ac^{3+}	F^-	2.008	2.021	−0.64	2,003.8	1,988.1	0.79
	Cl^-	2.480	2.486	−0.24	1,813.9	1,803.8	0.56
	HO^-	2.030	2.038	−0.39	2,119.4	2,107.0	0.59
	HS^-	2.488	2.494	−0.24	1,835.3	1,825.4	0.54
	CO	2.819	2.831	−0.42	191.7	188.5	1.70
m.p.d.				0.39			0.84
Cm^{3+}	F^-	1.942	1.916	1.36	2,119.0	2,150.4	−1.46
	Cl^-	2.369	2.339	1.28	1,967.7	1,993.8	−1.31
	HO^-	1.952	1.921	1.61	2,255.3	2,298.3	−1.87
	HS^-	2.370	2.340	1.28	1,994.4	2,027.3	−1.62
	CO	2.627	2.608	0.73	249.4	253.7	−1.69
m.p.d.				1.25			1.59
Lr^{3+}	F^-	1.871	1.885	−0.74	2,209.9	2,203.0	0.31
	Cl^-	2.292	2.294	−0.09	2,076.9	2,075.6	0.06
	HO^-	1.877	1.880	−0.16	2,357.0	2,355.5	0.06
	HS^-	2.280	2.276	0.18	2,090.6	2,091.5	−0.04
	CO	2.505	2.498	0.28	300.1	301.3	−0.40
m.p.d.				0.29			0.17

Basis sets: LPP (7s6p5d2f1g)/[5s4p3d2f1g]; SPP (14s13p10d8f6g)/[10s9p5d4f3g]; H, O, Cl, S, F contracted aug-cc-pVQZ

the rule derived by Schwarz and coworkers for the lanthanide contraction that soft bonds exhibit a more pronounced contraction than rigid ones [57]. Quite large actinide contractions (0.27–0.31 Å) are also observed for the tri- and tetraatomic ligands H_2S, H_2O and NH_3, whereas a smaller value (0.17 Å) is observed for NH_2^-. This is in agreement with the rule that a lower 5f contribution to bonding at the beginning of the series leads to a larger contraction (Mulliken f populations 0.00 for $Ac^{3+}CO$, and 0.05–0.07 for $Ac^{3+}H_2S$, $Ac^{3+}H_2O$, and $Ac^{3+}NH_3$ compared to 0.15–0.20 for $Ac^{3+}F^-$, $Ac^{3+}Cl^-$, $Ac^{3+}OH^-$, $Ac^{3+}SH^-$ and $Ac^{3+}NH_2^-$) [58].

The difference between the Cm systems exhibiting slightly too long bond lengths on one hand and the Ac and Lr systems with usually too short bond distances on the other hand is traced back to the half-occupied 5f shell of the trivalent Cm. It has to be noted that calculations with the Cm LPP do not correspond to the ground state, but rather to an average over all states belonging to a so-called superconfiguration [59], which includes all possible couplings within the partially occupied 5f shell. Besides the Cm^{3+} high-spin octet ground state, also, sextet, quartet, doublet and singlet states are described by the LPP. Since the latter have one or more electron pairs in the very compact 4f orbitals, the high electron repulsion leads to a larger radial extension and thus also to slightly longer bond distances in the LPP case compared to the SPP approach, which describes only the high-spin ground state. An investigation if LPPs can be adjusted which only describe the high-spin coupling in the open 5f shell might be worthwhile but is beyond the scope of the current study.

3.1.2 Binding energies

The LPP + CPP HF binding energies differ at most by 25.4 kJ mol^{-1} (1.3%, for $Lr^{3+}Cl^-$) from the corresponding SPP results, with the LPP + CPP values being usually higher than the SPP results. On average, the deviation for all 15 molecules is 12.5 kJ mol^{-1} (1.1%). At the LPP + CPP CCSD(T) level, the binding energies deviate by at most 43.0 kJ mol^{-1} (1.9%, for $Cm^{3+}HO^-$) from the SPP reference values. The average deviation amounts to 13.4 kJ mol^{-1} (0.9%). In contrast to the HF results, where the values for Cm deviate less than those for Ac and Lr, one finds at the CCSD(T) level the largest deviations for Cm, and smaller ones for Ac and Lr. The LPP + CPP values are higher than the SPP reference values for Ac and exhibit almost no deviations for Lr, whereas they are still underestimated for Cm. The lower binding energies for the Cm systems are in line with the longer bond distances and might be due to the same reason explained above.

Overall the HF and CCSD(T) LPP results of Ac and Lr exhibit smaller deviations of 0.8% in both cases, compared to those of Cm amounting to 1.3%. The performance of the Lr LPP + CPP at the CCSD(T) level for both bond lengths and binding energies is remarkably good, with average deviations of only 0.3 and 0.2%, respectively. The larger deviations at the HF level may partially be due to the usage of the CPP as explained above. For example, using the Lr LPP without CPP, one obtains at the HF level for $Lr^{3+}F^-$ a bond distance of 1.875 Å and a binding energy of 2141.9 kJ mol^{-1}, which agrees significantly better with the SPP results of 1.883 Å and 2145.5 kJ mol^{-1} than the results obtained at the LPP + CPP level of 1.862 Å and 2170.6 kJ mol^{-1}.

The binding energies calculated with wavefunction-based correlation approaches are certainly more difficult to calibrate than the bond distances, since they exhibit a higher sensitivity to the applied valence basis sets. Although the absolute deviations may appear to be quite large, it is noteworthy that the general trends caused by changes in the actinide ion or the ligand are very similar for LPP + CPP and SPP results.

3.2 Tetra- and pentaatomic systems

For the tetra- and pentaatomic systems $An^{3+}L^{n-}$ (An^{3+} = Ac^{3+}, Cm^{3+}, Lr^{3+}; L^{n-} = H_2O, H_2S, NH_2^-, NH_3) the CPC according to Eq. 9 could only be applied manually after the geometry optimization, i.e. only the binding energies and not the actinide-ligand bond lengths were corrected. The procedure was otherwise analogous to the one described above for the diatomic ligands, i.e. E_A^{AL} was evaluated using the equilibrium structure of the free ligand and the center carrying the ghost basis on the actinide was put at a distance corresponding the optimized metal-ligand distance in the complex.

For all tetraatomic $An^{3+}L^{n-}$ (n = 0,1) systems, C_{2v} equilibrium geometries were found. These correspond to a sp^2 hybridization at N, O and S, with one lone pair coordinating directly to the actinide ion and the other one located perpendicular to the molecular plane. In comparison with the free ligands, it is found that the H–X–H (X = O, S) angle for the neutral ligands increases upon complex formation, whereas it decreases for the anionic NH_2^- ligand. Analogously, the X-H bond lengths decrease for the neutral ligands and increase for NH_2^-. In the following discussion, we focus on the actinide-ligand distances. The HF and CCSD(T) results for the actinide-ligand bond distances and binding energies of the tetra- and pentaatomic systems are listed in Tables 3 and 4, respectively. Additional data, e.g. results for bond angles, are available in the supplementary material.

Table 3 Ac^{3+}–L^{n-} ($n = 0$, 1) bond lengths R_e (in Å) and binding energies D_e (in kJ mol^{-1}) from HF calculations using LPPs + CPPs as well as from SPP calculations tetra- and pentaatomic systems with CPC at the equilibrium geometry

An^{3+}	L^{n-}	R_e		$\frac{\Delta R_e}{R_e(SPP)}$	D_e		$\frac{\Delta D_e}{D_e(SPP)}$
		LPP	SPP		LPP	SPP	
Ac^{3+}	H_2O	2.436	2.449	−0.53	322.8	317.7	1.61
	H_2S	2.928	2.939	−0.37	261.5	257.4	1.59
	NH_2^-	2.165	2.170	−0.23	2,048.3	2,039.5	0.43
	NH_3	2.592	2.603	−0.42	360.5	356.0	1.26
m.p.d				0.39			1.22
Cm^{3+}	H_2O	2.272	2.281	−0.39	391.4	382.6	2.30
	H_2S	2.730	2.738	−0.29	340.4	330.1	3.12
	NH_2^-	2.065	2.050	0.73	2,220.3	2,217.2	0.14
	NH_3	2.417	2.421	−0.17	448.2	438.3	2.26
m.p.d				0.40			1.96
Lr^{3+}	H_2O	2.164	2.185	−0.96	444.3	429.8	3.37
	H_2S	2.617	2.631	−0.53	399.6	384.1	4.04
	NH_2^-	1.992	2.001	−0.45	2,334.7	2,308.8	1.12
	NH_3	2.312	2.327	−0.64	516.2	501.4	2.95
m.p.d				0.65			2.87

The relative deviations $\frac{\Delta R_e}{R_e(SPP)}$ and $\frac{\Delta D_e}{D_e(SPP)}$ are given in %. The mean (absolute) percentage deviation (m.p.d.) is given for the differences between LPP and SPP results

Basis sets: LPP (7s6p5d2f1g)/[5s4p3d2f1g]; SPP (14s13p10d8f6g)/[10s9p5d4f3g]; H, N, O, S contracted aug-cc-pVQZ

3.2.1 Actinide-ligand bond lengths

At the HF level, the calculated LPP + CPP bond lengths deviate from the SPP results by at most 0.021 Å (1.0%, for $Lr^{3+}H_2O$). As for the mono- and diatomic ligands, the LPP + CPP results for the Ac and Lr systems are slightly too short, whereas no unique trend can be discerned for the Cm complexes. On average the deviation for all 12 molecules is 0.011 Å (0.5%), which is almost identical to the deviations observed for the mono- and diatomic ligands.

At the CCSD(T) level, the maximum deviation is 0.050 Å (2.5%, for $Cm^{3+}NH_2^-$). The discrepancy for $Cm^{3+}NH_2^-$ is exceptionally large, so that the average deviation for all 12 molecules of only 0.019 Å (0.8%) is substantially smaller. Again the performance of the LPP + CPP approach is better for Ac and Lr than for Cm. The average deviations for the four ligands are at the HF and CCSD(T) level 0.3, 1.0 and 0.7% for Ac, Cm and Lr, respectively. The corresponding deviations for the four ligands H_2O, H_2S, NH_2^- and NH_3 amount to 0.6, 0.5, 0.8 and 0.7%, respectively.

The comparison between HF and CCSD(T) results shows that electron correlation shortens the actinide-ligand bond length in all cases for the SPP calculation. The LPP + CPP results, however, yield slightly longer bond distances for the $Cm^{3+}NH_2^-$ and $Lr^{3+}NH_2^-$ complexes. The reasons for this behavior cannot be explained at present.

Table 4 As Table 3, but for RCCSD(T) results

An^{3+}	L^{n-}	R_e		$\frac{\Delta R_e}{R_e(SPP)}$	D_e		$\frac{\Delta D_e}{D_e(SPP)}$
		LPP	SPP		LPP	SPP	
Ac^{3+}	H_2O	2.400	2.400	0.00	343.0	337.1	1.75
	H_2S	2.868	2.867	0.03	284.5	282.6	0.67
	NH_2^-	2.160	2.157	0.14	2,088.4	2,078.9	0.46
	NH_3	2.556	2.551	0.20	389.1	393.3	−1.07
m.p.d				0.09			1.00
Cm^{3+}	H_2O	2.254	2.224	1.35	408.9	414.7	−1.40
	H_2S	2.697	2.662	1.31	364.9	374.5	−2.56
	NH_2^-	2.073	2.023	2.47	2,254.6	2,296.9	−1.84
	NH_3	2.400	2.362	1.61	474.8	492.4	−3.57
m.p.d				1.69			2.34
Lr^{3+}	H_2O	2.150	2.139	0.51	463.3	460.7	0.56
	H_2S	2.591	2.574	0.66	426.1	425.9	0.05
	NH_2^-	2.000	1.982	0.91	2,368.6	2,372.9	−0.18
	NH_3	2.303	2.282	0.92	546.2	545.6	0.11
m.p.d				0.75			0.23

Basis sets: LPP (7s6p5d2f1g)/[5s4p3d2f1g]; SPP (14s13p10d8f6g)/[10s9p5d4f3g]; H, N, O, S contracted aug-cc-pVQZ

The difference between the Ac and Lr bond distances, i.e. the actinide contraction, obtained at the SPP level is reproduced by the LPP + CPP results with maximum deviations of 0.008 and 0.016 Å at the HF and CCSD(T) level, respectively. The size of the actinide contraction follows the order $H_2S > NH_3$, $H_2O \gg NH_2^-$, in accordance with the finding that for a large 5f participation at the beginning of the actinide row a small actinide contraction is observed [58]. The Ac Mulliken f population in $Ac^{3+}NH_2^-$ of 0.19 electrons is significantly larger than those in $Ac^{3+}H_2O$, $Ac^{3+}NH_3$ and $Ac^{3+}H_2S$ of 0.06, 0.05 and 0.07, respectively, in agreement with the actinide contraction of the $An^{3+}NH_2^-$ complexes amounting to only 55–65% of the one found for the other three systems. $An^{3+}NH_2^-$ behaves similar to the other complexes with charged ligands, i.e. $An^{3+}F^-$, $An^{3+}Cl^-$, $An^{3+}OH^-$ and $An^{3+}SH^-$, which exhibit an intermediate actinide contraction and a substantial 5f participation in bonding at the beginning of the series.

3.2.2 Binding energies

The LPP + CPP HF binding energies are for most systems larger than the SPP values, with a maximum difference of 25.9 mol^{-1} (1.1%, for $Lr^{3+}NH_2^-$). The average deviation for all 12 molecules is 10.4 kJ mol^{-1} (2.0%). The relative deviations increase from Ac (1.2%) over Cm (2.0%) to Lr (2.9%). As discussed above, the discrepancies may be

partly related to the usage of CPPs in the LPP calculations, which besides correctly accounting for static core-polarization effects also describe dynamic core polarization which is not present in the SPP HF reference calculations. For example, the results for $Lr^{3+}H_2O$ obtained at the LPP level without a CPP of 2.186 Å and 427.2 kJ mol^{-1} agree again better with the SPP HF values of 2.185 Å and 429.8 kJ mol^{-1} than the LPP + CPP results of 2.164 Å and 444.3 kJ mol^{-1}.

At the CCSD(T) level, the largest absolute deviation between LPP + CPP and SPP results is 42.3 kJ mol^{-1} (1.8%, for $Cm^{3+}NH_2^-$), and the largest relative one is 3.6% (17.6 kJ mol^{-1}, for $Cm^{3+}NH_3$). The average deviation for all 12 molecules is 8.7 kJ mol^{-1} (1.2%). Again the performance of the Lr LPP + CPP is very good at the CCSD(T) level with average deviations of only 0.8 and 0.2% for bond lengths and binding energies, respectively. For the Ac systems, the LPP + CPP approach yields slightly too high binding energies, whereas they turn out to be too low for the Cm systems. Overall the HF and CCSD(T) LPP + CPP results exhibit deviations of 1.1, 2.1 and 1.5% for Ac, Cm and Lr, respectively.

3.3 Density functional calculations

Since a very large part of computational chemistry is performed at the DFT level whereas the PPs presented here were derived in the framework of HF, and since most of the electronic structure codes cannot handle CPPs, we performed additional calculations using the LPPs without CPPs at the BP86 [45, 46], B3LYP [47–50] and PBE0 [51] DFT levels in order to establish the errors resulting from such an approach. The performance of HF-derived large-core PPs within DFT calculations was frequently found to be poor [29, 60] and even for DFT-based PPs used in solid-state physics a nonlinear core correction was recommended [61]. A detailed summary of the results is given in the supplementary material. In the following, we only discuss the errors observed at the DFT LPP level in comparison with the CCSD(T) LPP + CPP results. For bond lengths, the deviations are listed in Table 5. On the average, they amount to 0.7, 0.4 and 0.2 % for B3LYP, BP86 and PBE0. For the B3LYP and BP86 functionals, the LPP bond distances are consistently shorter than the CCSD(T) LPP + CPP results, whereas for the PBE0 functional slightly longer bond distances are obtained. In all cases, the deviations stay below 1.2 % and indicate that the LPPs can be used in DFT calculations for structure optimizations.

Table 6 summarizes the corresponding errors for the binding energies. The average relative deviations of the LPP B3LYP, BP86 and PBE0 values from the CCSD(T) LPP + CPP results are 2.1, 4.7 and 3.5%, respectively. The largest deviations occur for the H_2S adducts and amount to 8.6, 13.4 and 11.0% for B3LYP, BP86 and PBE0, respectively. These deviations are significantly larger than those observed between SPPs and LPPs at the HF and CCSD(T) level. If corrections for the omitted core electron density [61] would improve the results has to be investigated.

Table 5 Errors (%) of An^{3+}–L^{n-} ($n = 0, 1$) bond distances from 5f-in-core DFT calculations without CPP in comparison with corresponding CCSD(T) results obtained with CPPs

L^{n-}	An^{3+}	B3LYP	BP86	PBE0
F^-	Ac^{3+}	0.45	0.35	−0.35
	Cm^{3+}	0.62	0.67	−0.10
	Lr^{3+}	0.64	0.69	−0.05
Cl^-	Ac^{3+}	0.52	0.16	−0.40
	Cm^{3+}	0.59	0.38	−0.30
	Lr^{3+}	0.65	0.39	−0.26
HO^-	Ac^{3+}	0.30	0.15	−0.49
	Cm^{3+}	0.51	0.51	−0.26
	Lr^{3+}	0.37	0.37	−0.32
HS^-	Ac^{3+}	0.48	0.16	−0.52
	Cm^{3+}	0.51	0.38	−0.38
	Lr^{3+}	0.53	0.39	−0.26
CO	Ac^{3+}	0.74	−0.11	−0.18
	Cm^{3+}	0.88	0.27	0.11
	Lr^{3+}	1.00	0.48	0.29
H_2O	Ac^{3+}	0.63	0.00	−0.33
	Cm^{3+}	0.89	0.49	0.04
	Lr^{3+}	0.84	0.56	0.14
H_2S	Ac^{3+}	0.98	0.28	−0.24
	Cm^{3+}	1.19	0.82	0.07
	Lr^{3+}	1.08	0.73	0.08
NH_2^-	Ac^{3+}	0.60	0.46	−0.32
	Cm^{3+}	0.58	0.58	0.24
	Lr^{3+}	0.45	0.35	−0.35
NH_3	Ac^{3+}	0.82	0.23	−0.35
	Cm^{3+}	1.03	0.62	0.00
	Lr^{3+}	1.09	0.65	−0.04
m.p.d.		0.70	0.42	0.24

3.4 Overview

The trends in the actinide-ligand distances for $An^{3+}L^{n-}$ ($n = 0, 1$) are graphically displayed in Fig. 1. It can be seen that both the trends for a change in the ligands and for a change in the actinide ion are very similar for LPP + CPP and SPP at the CCSD(T) level. The small deviations for the bond distances for the Cm systems are visible, whereas almost identical curves are obtained for Ac and Lr. It can also be seen that the actinide contraction is

Table 6 Errors (%) of An^{3+}–L^{n-} ($n = 0, 1$) binding energies from 5f-in-core DFT calculations without CPP in comparison with corresponding CCSD(T) results obtained with CPPs

L^{n-}	An^{3+}	B3LYP	BP86	PBE0
F^-	Ac^{3+}	−0.15	0.96	1.09
	Cm^{3+}	−0.03	1.19	0.85
	Lr^{3+}	0.20	1.32	0.88
Cl^-	Ac^{3+}	0.19	1.81	1.47
	Cm^{3+}	0.59	2.26	1.44
	Lr^{3+}	0.78	2.21	1.30
HO^-	Ac^{3+}	4.09	5.01	5.11
	Cm^{3+}	4.03	5.04	4.67
	Lr^{3+}	4.01	4.90	4.46
HS^-	Ac^{3+}	0.05	1.71	1.45
	Cm^{3+}	0.54	2.26	1.48
	Lr^{3+}	0.74	2.29	1.43
CO	Ac^{3+}	0.26	7.98	3.81
	Cm^{3+}	1.28	8.38	3.37
	Lr^{3+}	1.73	7.66	2.77
H_2O	Ac^{3+}	1.95	4.29	4.20
	Cm^{3+}	2.35	4.72	3.64
	Lr^{3+}	2.59	4.55	3.35
H_2S	Ac^{3+}	7.28	12.55	11.04
	Cm^{3+}	8.28	13.43	10.33
	Lr^{3+}	8.59	12.70	9.72
NH_2^-	Ac^{3+}	0.02	0.90	1.41
	Cm^{3+}	0.37	1.34	1.37
	Lr^{3+}	0.66	1.47	1.38
NH_3	Ac^{3+}	1.98	5.01	4.99
	Cm^{3+}	2.40	5.27	4.34
	Lr^{3+}	2.58	4.78	3.66
m.p.d.		2.14	4.67	3.52

larger for the first half (Ac–Cm) of the series than for the second half (Cm–Lr).

The corresponding trends in the actinide-ligand binding energies D_e are shown in Fig. 2. As for the bond distances, the trends of the SPP CCSD(T) reference values for a change in the actinide ion or the ligand are quite well reproduced by the LPP + CPP results. The binding energies of the complexes with ionic ligands increase from Ac over Cm to Lr, essentially in parallel to the corresponding bond distance contraction and the concomitant increased ionic attraction, whereas the differences are smaller for the uncharged ligands.

Finally, it has to be pointed out that the 5f-in-core LPP approach is computationally much more simple than the 5f-in-valence SPP or a corresponding relativistic AE approach. The elimination of the open 5f shell renders all systems studied here to be of closed-shell character. This would also be true for actinide elements other than Ac, Cm and Lr, where for an explicit treatment of the 5f shell a larger number of near-degenerate low-lying states may be present. Besides the computational difficulty to find and converge the lowest state, often also a multi-configurational treatment would be required, thus excluding black-box single-reference methods such as CCSD, CCSD(T) or DFT at the SPP or AE level. These methods are applicable without problems when using LPPs.

3.5 The U(III) complex $(C_5H_5)_3UCO$

In this last section, we comment briefly on a spectacular failure of the actinide 5f-in-core LPP approach recently reported in the literature. Maron and coworkers studied CO adducts to various U(III) complexes $Cp'_3U(CO)$

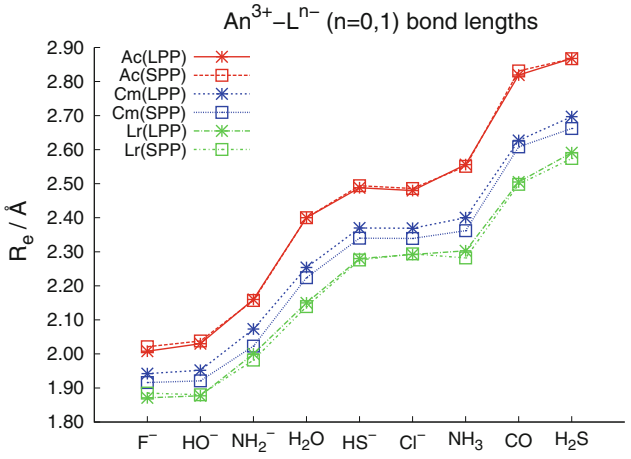

Fig. 1 An^{3+}–L^{n-} ($n = 0, 1$) distances from SPP and LPP + CPP CCSD(T). Basis sets: LPP (7s6p5d2f1g)/[5s4p3d2f1g]; SPP (14s13p10d8f6g)/[10s9p5d4f3g]; H, N, O, Cl, S, F contracted aug-cc-pVQZ

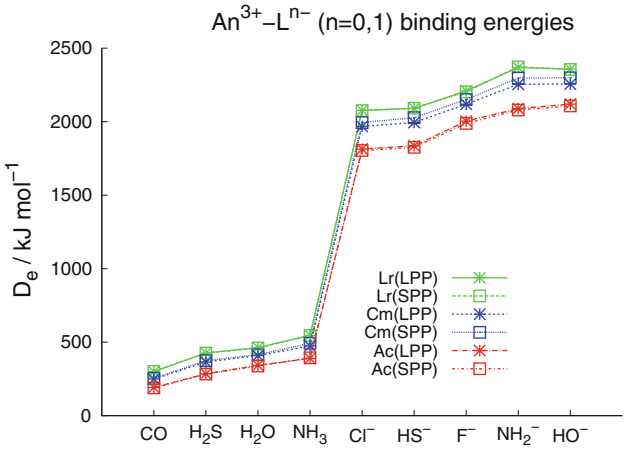

Fig. 2 An^{3+}–L^{n-} ($n = 0, 1$) binding energies from SPP and LPP + CPP CCSD(T) calculations. Basis sets: LPP (7s6p5d2f1g)/[5s4p3d2f1g]; SPP (14s13p10d8f6g)/[10s9p5d4f3g]; H, N, O, Cl, S, F contracted aug-cc-pVQZ

($Cp' = C_5H_{5-n}(CH_3)_n$) using a U $5f^3$-in-core LPP and a 5f-in-valence SPP at the DFT level [41]. The LPP approach was found to lead to too weak U–CO and U–Cp' bonding and significantly too long corresponding bond distances when compared to the SPP results, which were found to agree reasonably well with experimental data. At the LPP level, the U-ring distances were 0.08–0.40 Å and the U–CO distances 0.18–0.29 Å too long. The failure of the LPP was explained by the fact that the σ U–CO bond cannot be formed properly, since the 5f shell is included in the core.

In order to further investigate the reasons for the failure of the U(III) $5f^3$-in-core LPP, we performed test calculations on UCO^{3+}, UCp^{2+} and Cp_3UCO using both a U LPP and SPP at the BP86 DFT, MCSCF and CCSD(T) level with the MOLPRO program [53]. For all three systems, the U center is assumed to be trivalent and to have a $5f^3$ configuration. Here, we only discuss results from a Mulliken population analysis at the BP86 DFT level, cf. Table 7. Additional information is available from the supplementary material. Using a generalized contracted SPP basis set [25], we can distinguish between the f and the 5f population on U. Moreover, for each of these, we can distiguish values referring to all occupied orbitals and to the three singly occupied orbitals only. A successful application of the U(III) $5f^3$-in-core LPP requires the presence of three electrons in the 5f shell, e.g. a minimum 5f population of about three for the singly occupied orbitals. Table 7 reveals that this requirement is approximately fulfilled for UCO^{3+} and UCp^{2+}, thus explaining the reasonable agreement of the SPP and LPP U–C bond distances (UCO^{3+} SPP:2.655 Å; LPP:2.740 Å; UCp^{2+} SPP:2.616 Å, LPP:2.674 Å). In case of Cp_3UCO, however, the U 5f population for the three singly occupied orbitals is only 2.40 charge units. In contrast to UCO^{3+} and UCp^{2+}, where the U f character of each of the three singly occupied orbitals is higher than 99 and 96%, respectively, it amounts only to 91, 79 and 77% for Cp_3UCO. Therefore, despite the total Mulliken U f population of 3.17 charge units, Cp_3UCO is not suitable for the application of a U(III) $5f^3$-in-core LPP.

Table 7 Mulliken f and 5f populations for UCO^{3+}, UCp^{2+} and Cp_3UCO obtained from SPP calculations using generalized contracted basis sets at the BP86 DFT level

system	*n*(f)	*n*(5f)
UCO^{3+}	3.07/2.99	3.05/2.98
UCp^{2+}	3.18/2.90	3.14/2.89
Cp_3UCO	3.17/2.41	2.97/2.40

The values .../... refer to all orbitals/only the three singly occupied orbitals

4 Conclusion

5f-in-core LPPs and corresponding CPPs were calibrated against 5f-in-valence SPP results for a series of actinide-ligand model systems $An^{3+}L^{n-}$ ($n = 0$, 1) in HF and CCSD(T) calculations using basis sets of quadruple-zeta quality. For all linear model systems, the 5f-in-core LPP HF and CCSD(T) results show good agreement with the corresponding 5f-in-valence SPP reference data, i.e. the mean deviations of the absolute (relative) values in HF and CCSD(T) results amount for metal-ligand bond lengths to 0.011 Å (0.5%) and 0.014 Å (0.6%), respectively. For the metal-ligand binding energies, the corresponding average deviations are 12.5 kJ mol^{-1} (1.1%) and 13.4 kJ mol^{-1} (0.9%). The results for the nonlinear model systems are of the same quality, i.e. mean deviations of the absolute (relative) values for the metal-ligand bond distances and binding energies are for HF 0.011 Å (0.5%) and 10.4 kJ mol^{-1} (2.0%), respectively. The corresponding CCSD(T) values are 0.019 Å (0.8%) and 8.7 mol^{-1} (1.2%). The performance of the LPPs without CPPs was also investigated at the DFT level using the BP86, B3LYP and PBE0 functionals, where LPP + CPP CCSD(T) actinide-ligand bond distances were reproduced with average errors of 0.6% or less. On the whole, the 5f-in-core LPP(+CPP) approach can be expected to reproduce bond distances and binding energies evaluated with the more rigorous 5f-in-valence SPPs within 1–2% accuracy. In addition, the LPP(+CPP) results reproduce the trends of the SPP reference values very well, e.g. the changes occuring upon substitution of the actinide ion or the ligand. In view of the fact that studies on larger systems usually are performed at the DFT level and use smaller basis sets, the errors caused by the computationally very simple 5f-in-core LPPs may be still acceptable for many purposes. In any case, before applying the 5f-in-core approach, it should be carefully investigated by a test calculation treating 5f explicitly if the 5f occupation in the system of interest is consistent with the one assumed by the LPP.

References

1. Kaltsoyannis N, Hay PJ, Li J, Blaudeau JP, Bursten BE (2008) In: Morss LR, Edelstein N, Fuger J (eds) The chemistry of the actinide and transactinide elements, 3rd edn. Springer Dordrecht, The Netherlands, p 1893
2. Abu-Khader MM (2009) Prog Nucl Energy 51:225
3. Pyykkö P (1987) Inorg Chim Acta 139:243
4. Pepper M, Bursten BE (1991) Chem Rev 91:719
5. Schreckenbach G, Hay PJ, Martin RL (1999) J Comp Chemn 20:70
6. Dolg M, Cao X (2004) In: Hirao K, Ishikawa Y (eds) Recent advances in relativistic molecular theory, vol 6, ed. (World Scientific, New Jersey, 2004), chap 1
7. Pyykkö P (1988) Chem Rev 88:563

8. Cao X, Dolg M (2006) Coord Chem Rev 250:900
9. Schwerdtfeger P, Brown JR, Laerdahl JK, Stoll H (2000) J Chem Phys 113:7110
10. Peterson KA, Puzzarini C (2005) Theor Chem Acc 114(4–5):283
11. Cao X, Dolg M (2010) In: Barysz M, Ishikawa Y (eds) Challenges and advances in computational chemistry and physics, vol 10, (CRC-Press, New York, 2010), chap. 6
12. Weigand A, Cao X, Vallet V, Flament JP, Dolg M (2010) J Phys Chem 113(43):11509
13. Cao X, Dolg M (2009) J Phys Chem A 113:12573
14. Dolg M, Stoll H, Savin A, Preuss H (1989) Theor Chim Acta 75:173
15. Dolg M, Stoll H, Preuss H (1993) Theor Chim Acta 85:441
16. Wang Y, Dolg M (1998) Theor Chem Acc 100:124
17. Hülsen M, Weigand A, Dolg M (2009) Theor Chem Acc 122:23
18. Moritz A, Cao X, Dolg M (2007) Theor Chem Acc 117:473
19. Moritz A, Cao X, Dolg M (2007) Theor Chem Acc 118:845
20. Moritz A, Dolg M (2008) Theor Chem Acc 121:297
21. Dolg M, Stoll H, Preuss H (1989) J Chem Phys 90:1730
22. Küchle W, Dolg M, Stoll H, Preuss H (1994) J Chem Phys 100:7535
23. Cao X, Dolg M (2001) J Chem Phys 115(16):7348
24. Cao X, Dolg M (2002) J. Molec. Struct. (Theochem) 581:139
25. Cao X, Dolg M, Stoll H (2003) J Chem Phys 118:487
26. Cao X, Dolg M (2004) J Molec Struct (Theochem) 673:203
27. Müller W, Flesch J, Meyer W (1984) J Chem Phys 80:3297
28. Müller W, Meyer W (1984) J Chem Phys 80:3311
29. Jong WAD, Harrison RJ, Nichols JA, Dixon DA (2001) Theor Chem Acc 107:22
30. Vallet V, Macak P, Wahlgren U, Grenthe I (2006) Theor Chem Acc 115(2–3):145
31. Odoh SO, Schreckenbach G (2010) J Phys Chem A 114(4):1957
32. Schreckenbach G, Shamov GA (2010) Acc Chem Res 43(1):19
33. Iché-Tarrat N, Marsden CJ (2008) J Phys Chem 112:7632
34. Weigand A, Cao X, Yang J, Dolg M (2010) Theor Chem Acc 126:117
35. Wiebke J, Moritz A, Cao X, Dolg M (2007) Phys Chem Chem Phys 9:459
36. Skerencak A, Panak PJ, Neck V, Trumm M, Schimmelpfennig B, Lindqvist-Reis P, Klenze R, Fanghaenel T (2010) J Phys Chem B 114(47):15626
37. Cao X, Li Q, Moritz A, Xie Z, Dolg M, Chen X, Fang W (2006) Inorg Chem 45(8):3444
38. Cao X, Heidelberg D, Ciupka J, Dolg M (2010) Inorg Chem 49:10307
39. Castro L, Yahia A, Maron L (2010) Dalton Trans 39:6682
40. Castro L, Yahia A, Maron L (2010) Phys Chem Phys 11:990
41. Maron L, Eisenstein O, Andersen RA (2009) Organometallics 28:3629
42. Banik NL, Schimmelpfennig B, Marquardt CM, Brendebach B, Geist A, Denecke MA (2010) Dalton Trans 39:5117
43. Wood JH, Boring AM (1978) Phys Rev B 18:2701
44. Kendall RA, Dunning TH Jr., Harrison RJ (1992) J Chem Phys 96:6796
45. Becke AD (1986) J Chem Phys 84(8):4524
46. Perdew JP (1986) Phys Rev B 33:8822
47. Becke AD (1993) J Chem Phys 98:5648
48. Becke AD (1988) Phys Rev A 38:3098
49. Lee C, Yang W, Parr RG (1988) Phys Rev B 37(2):785
50. Vosko SH, Wilk L, Nusair M (1980) Can J Phys 58:1200
51. Adamo C, Barone V (1999) J Chem Phys 110(13):6158
52. Deegan MJO, Knowles PJ (1994) Chem Phys Lett 227:321
53. Werner HJ, Knowles PJ, Lindh R, Manby FR, Schütz M, Celani P, Korona T, Mitrushenkov A, Rauhut G, Adler TB, Amos RD, Bernhardsson A, Berning A, Cooper DL, Deegan MJO, Dobbyn AJ, Eckert F, Goll E, Hampel C, Hetzer G, Hrenar T, Knizia G, Köppl C, Liu Y, Lloyd AW, Mata RA, May AJ, McNicholas SJ, Meyer W, Mura ME, Nicklass A, Palmieri P, Pflüger K, Pitzer R, Reiher M, Schumann U, Stoll H, Stone AJ, Tarroni R, Thorsteinsson T, Wang M, Wolf A, Molpro A version 2006.1, a package of ab initio programs (2006)
54. Knowles PJ, Hampel C, Werner HJ (1993) J Chem Phys 99:5219
55. Boys SF, Bernardi F (1970) Mol Phys 19:553
56. Leininger T, Nicklass A, Stoll H, Dolg M, Schwerdtfeger P (1996) J Chem Phys 105:1052
57. Wang SG, Schwarz WHE (1995) J Phys Chem 99:11687
58. Dolg M, Stoll H, (1996) Elsevier, pp 607–729
59. Field RW (1982) Ber Bunsenges Phys Chem 86(9):771
60. Russo TV, Martin RL, Hay PJ (1995) J Phys Chem 99:17085
61. Louie SG, Froyen S, Cohen ML (1982) Phys Rev B 26(4):1738